AIM Studies on Reactions FNCX → FXCN (X = O, S, and Se)

Yanli Zeng,[†,‡] Shijun Zheng,*[,†,‡] and Lingpeng Meng[†]

Institute of Computational Quantum Chemistry, College of Chemistry, Hebei Normal University, Shijiazhuang 050091, P. R. China, and Department of Chemistry, Graduate School, Chinese Academy of Sciences, Beijing 100039, P. R. China

Received: June 22, 2004; In Final Form: September 8, 2004

The reactions of FNCO to FOCN, FNCS to FSCN, and FNCSe to FSeCN have been studied at MP2/6-311++G (2df)//B3LYP/6-311++G (2df) level. Geometries of the reactants, transition states, intermediates, and products have been optimized. The reason that FSCN is easily detected instead of FNCS has been explained. We predict that FNCO and FSeCN are more easily detected than FOCN and FNCSe, respectively. The breaking and formation of the chemical bonds in the reactions have been discussed by the topological analysis method of electronic density. The calculated results show that there are two kinds of structure transition states (the T-shaped conflict structure transition state and the bifurcation-type ring structure transition state) in the reactions studied.

1. Introduction

For those molecules of the series that contain OCN, SCN, and SeCN fragments, a complication that arises is that the remaining group can, in principle, be bonded to both ends of the fragment. From the photoelectron spectrum (PES) study of the compounds XNCO (X = Cl, Br, and I), it has been shown that in these cases bonding occurs through the nitrogen atom.[1−3] The molecules XSCN (X = F, Cl, Br, and I)[3−6] and XSeCN (X = Cl, Br, and I)[3,7] have also been studied using PES, but no evidence for the bonding through the nitrogen atom was detected.

As we know, judging the breaking or formation of a bond is almost impossible with experimental methods and traditional population analysis. According to the theory of "atoms in molecules (AIM)", topological studies on reaction paths of some typical reactions have been carried out by some authors in recent years,[8−17] but much more are still to be known about the relationship between topological characteristics of density distribution and the energy variation along the reaction path.

In this paper, we carried out studies on the reactions FNCX → FXCN (X = O, S, and Se), trying to explain the reason that the fluorine atom is bonded to the SCN group only through S, and predict that FNCO and FSeCN are more stable and easily detected than FOCN and FNCSe, respectively, just as ClNCO, BrNCO, and INCO are more easily detected than ClOCN, BrOCN, and IOCN and ClSeCN, BrSeCN, and ISeCN are more easily detected than ClNCSe, BrNCSe, and INCSe, respectively. The geometries of the energy transition states and intermediates of the three reactions are found for the first time. The breaking and formation of the bonds in the isomerization reaction paths have been discussed, and the T-shaped conflict structure transition state and the bifurcation-type ring structure transition state have been found in the reactions studied. This paper is an extension and further example of the established ideas and concepts of AIM.[8−12]

* To whom correspondence should be addressed. E-mail: sjzheng@mail.hebtu.edu.cn.

† Hebei Normal University.

‡ Chinese Academy of Sciences.

2. Computational Methods

The geometries of reactants, transition states, intermediates, products, and every point on the potential energy surface were located by B3LYP calculations with second-order MP2 energy corrections as well as zero-point energy corrections, using the 6-311++G(2df) basis set. Starting from the transition state, the reaction path has been followed using Fukui's theory of the intrinsic reaction coordinate (IRC) method[18] in mass-weighted internal coordinates going in forward and reverse directions from the transition state with the step size equaled to 0.01 $(amu)^{1/2}$bohr. In this work, the reaction paths were traced out by the mass-weighted internal coordinate (S), which is more precise than a single distance or an angle.[19,20] The computations were performed using the Gaussian 98 program.[21] Topological analyses were carried out with program AIM 2000.[22] The structures (Figure 1) and gradient paths of the electronic density on the IRC path of FNCX → FXCN (X = O, S, and Se; Figures 3−5) were plotted by program AIM 2000.[22]

3. Results and Discussion

3.1. Potential Energy Curves on IRC Paths. The geometry parameters of the reactants, transition states, intermediates, and products on the potential energy surfaces have been optimized and listed in Table 1. As an example of the topic series reactions, we illustrate the structures of FNCS, FSCN, the intermediate (IM), and their transition states (TSa and TSb) in Figure 1. All of the geometries and structures have C_s symmetry; that is, the four atoms are in the same plane in the reactions paths all along. The geometries of the intermediates and the transition states are found for the first time. The frequencies were computed using the analytical second derivatives in order to check that the stationary points exhibit the proper number of imaginary frequencies: none for a minimum and one for a transition state (first-order saddle point). IRC calculations were carried out to validate the connection of the reactants (FNCX), transition states, intermediates, and products (FXCN) (X = O, S, and Se). Along the reaction paths, there is no breaking at the N−C bond or the C−X (X = O, S, and Se) bond. The F−N bond is broken, the F−C bond appears, and the F−X (X = O, S, and Se) bond

10.1021/jp0472865 CCC: $27.50
Published on Web 10/30/2004

TABLE 1: Optimized Geometry Parameters at B3LYP/6-311++G(2df) Level[a]

	FNCO	FNCS	FNCSe
B(F−N)/Å	1.4032	1.4040	1.4057
B(N−C)/Å	1.2433	1.2326	1.2275
B(C−X)/Å	1.1558	1.5527	1.6996
A(CNF)/°	113.0	115.0	116.1
A(XCN)/°	170.1	171.6	171.3
D(XNCF)/°	180.0	180.0	180.0
	TSa	TSa	TSa
B(F−C)/Å	1.4314	1.6009	1.6785
B(N−C)/Å	1.2953	1.2427	1.2254
B(X−C)/Å	1.1815	1.5911	1.7412
A(NCF)/°	92.5	82.1	79.9
A(XCF)/°	125.9	127.1	126.9
D(XCFN)/°	180.0	180.0	180.0
	IM	IM	IM
B(F−C)/Å	1.2976	1.2987	1.3007
B(N−C)/Å	1.2612	1.2356	1.2307
B(X−C)/Å	1.2533	1.7074	1.8657
A(NCF)/°	134.3	136.8	136.5
A(XCF)/°	127.9	137.9	138.7
D(XCFN)/°	180.	180.	180.0
	TSb	TSb	TSb
B(F−C)/Å	2.0118	1.7156	1.6991
B(N−C)/Å	1.2121	1.1953	1.1906
B(X−C)/Å	1.1850	1.6324	1.7900
A(NCF)/°	106.5	123.1	124.7
A(XCF)/°	75.4	85.5	85.2
D(XCFN)/°	180.0	180.0	180.0
	FOCN	FSCN	FSeCN
B(F−X)/Å	1.4731	1.6304	1.7645
B(C−X)/Å	1.2819	1.6800	1.8352
B(N−C)/Å	1.1579	1.1578	1.1562
A(CXF)/°	106.9	100.1	97.7
A(NCX)/°	175.1	176.1	175.8
D(NCXF)/°	180.0	180.0	180.0

[a] B denotes bond length, A denotes bond angle, and D denotes dihedral.

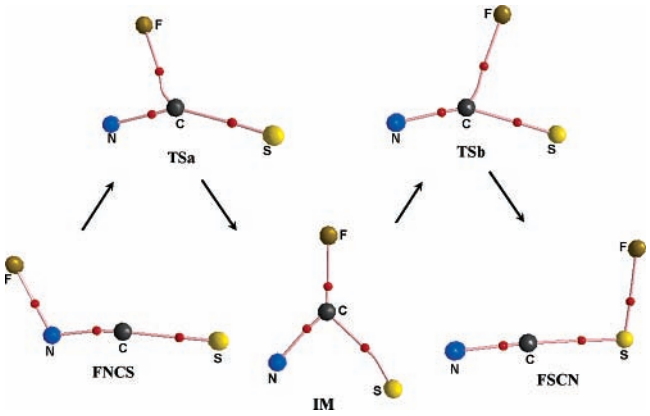

Figure 1. Displays of Structures of FNCS, FSCN, intermediate and transition states. Bond critical points are shown as small circle sphere.

forms. As the F−C bond disappears, the F−X (X = O, S, and Se) bond becomes stronger.

The potential energy curves of the topic reactions are given in Figure 2. On the basis of B3LYP optimized geometries, the energies are corrected by B3LYP zero-point energy corrections and second-order MP2 energy corrections, respectively. All of the calculations are at the 6-311++G(2df) basis set level. The energies calculated by both methods have the same trends.

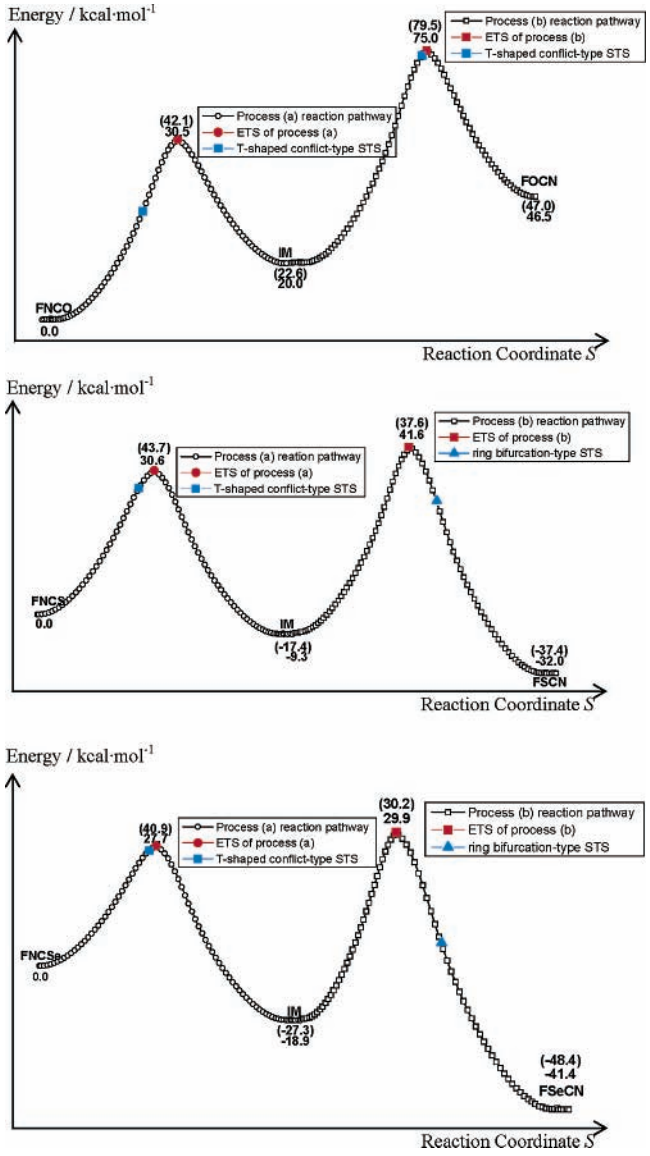

Figure 2. Potential energy curves of FNCX → FXCN (X = O, S, and Se) reactions. Energies in parentheses are MP2 corrected energies, and the energies below are corrected by zero-point energies.

There are two steps in each of the topic reactions: the first step is FNCX → TSa → IM, and the second step is IM → TSb → FXCN (X = O, S, and Se). The two steps of the FNCO → FOCN process are both endothermic. If the fluorine atom is bonded to the OCN group through the O atom, it is very easy for FOCN to isomerize to FCNO (IM) and for FCNO (IM) to isomerize to FNCO. On the contrary, if the fluorine atom is bonded to the OCN group through the N atom, it is difficult for FNCO to isomerize to FCNO (IM) and for FCNO (IM) to isomerize to FOCN. The two steps of the FNCS → FSCN and FNCSe → FSeCN processes are both exothermic. If the fluorine atom is bonded to the SCN or SeCN group through the S or Se atom, it is difficult for FSCN or FSeCN to isomerize to FCNS (IM) or FCNSe (IM) and for FCNS (IM) or FCNSe (IM) to isomerize to FNCS or FNCSe. On the contrary, if the fluorine atom is bonded to the SCN or SeCN group through the N atom, it is very easy for FNCS or FNCSe to isomerize to FCNS (IM) or FCNSe (IM) and for FCNS (IM) or FCNSe (IM) to isomerize to FSCN or FSeCN.

The Gibbs free energies are calculated at the B3LYP/6-311++G(2df) level with thermal corrections and summarized in Table 2. It is well known that, for a reaction, if $\Delta G < 0$, the

TABLE 2: Gibbs Free Energies on the FNCX → IM → FXCN (X = O, S, and Se) Pathway

	FNCX/ (a.u.)	IM/ (a.u.)	FXCN/ (a.u.)	FNCX → IM/ (kcal/mol)	IM → FXCN/ (kcal/mol)	FNCX → FXCN/ (kcal/mol)
X = O	−267.92523	−267.89319	−267.85100	20.1	26.5	46.6
X = S	−590.89154	−590.90616	−590.94275	−9.2	−23.0	−32.1
X = Se	−2594.21626	−2594.24615	−2594.28256	−18.8	−22.8	−41.6

TABLE 3: Electronic Densities $\rho(r_c)$ at the Critical Points on the FNCO → FOCN Pathway

S [a,b]/(amu)$^{1/2}$bohr	F−N	F−BCP(N−C)	F−C	F−BCP(C−O)	F−O	N−C	C−O
FNCO	0.2873					0.4229	0.4720
$S_a = -2.30$	0.1345					0.4168	0.4814
$S_a = -2.20$ (STS)		0.1358				0.4163	0.4809
$S_a = -2.10$			0.1377			0.4154	0.4808
$S_a = -0.00$ (TSa, ETS)			0.2258			0.3984	0.4562
IM			0.3090			0.4177	0.3892
$S_b = -0.31$			0.0590			0.4451	0.4502
$S_b = -0.30$ (STS)				0.0589		0.4453	0.4500
$S_b = -0.29$					0.0589	0.4454	0.4499
$S_b = 0.00$ (TSb, ETS)					0.0577	0.4507	0.4438
FOCN					0.2479	0.4802	0.3545

[a] S, reaction coordinate. [b] −, denotes reverse direction of the reaction.

reaction may occur spontaneously, and if $\Delta G > 0$, the reaction cannot occur spontaneously. The Gibbs free energy changes of the FNCO → FCNO(IM) and FCNO(IM) → FOCN processes are both less than zero, so then, the above processes cannot occur spontaneously. The Gibbs free energy changes of the FNCX → FCNX(IM) and FCNX(IM) → FXCN (X = S and Se) processes are both more than zero. Then the above process may occur spontaneously. Therefore, FSCN instead of FNCS is detected in the UPS experiments, and we predict that FNCO and FSeCN will be more easily detected than FOCN and FNCSe, just as ClNCO, BrNCO, and INCO are more easily detected than ClOCN, BrOCN, and IOCN, ClSeCN and BrSeCN and ISeCN are more easily detected than ClNCSe, BrNCSe, and INCSe, respectively.

3.2. Topological Analyses of Electronic Density on IRC Paths. For each reaction, the topological analysis was carried out on the electronic density of every point along the reaction path. Topological properties are listed in Tables 3−5 for FNCX → FXCN (X = O, S, and Se), respectively. Gradient paths of the electronic density are plotted for some points along the IRC path and displayed in Figures 3−5 for FNCX → FXCN (X = O, S, and Se), respectively.

3.2.1. Changes in Structure Determined by the Topology of the Electron Density. According to the topological analysis of electronic density distribution in the theory of atoms in molecules (AIM)[11,23] $\rho(\boldsymbol{r}_c)$ is used to describe the strength of a bond and $\nabla^2\rho(\boldsymbol{r}_c)$ is used to describe the characteristic of the bond. In general, the larger the value of $\rho(\boldsymbol{r}_c)$, the stronger the bond. The field of $\nabla^2\rho(\boldsymbol{r}_c) < 0$ is a charge accumulated area, and $\nabla^2\rho(\boldsymbol{r}_c) > 0$ is a charge dispersed area. $\nabla^2\rho(\boldsymbol{r}_c) = \lambda_1 + \lambda_2 + \lambda_3$, λ_i is an eigenvalue of the Hessian matrix of ρ, and $\boldsymbol{r}_c$ is the critical point (called saddle point) on the electronic density surface, and it is connected by two gradient paths (called bond paths) forming the bond that connects the two nuclei. Then, when one of the three λ_i's is positive and the other two are negative, we denote it by (3, −1) and call it the bond critical point (BCP). When one of the three λ_i's is negative and the other two are positive, we denoted it by (3, +1) and call it the ring critical point (RCP), which indicates that a ring structure exists. For the RCP, the single negative curvature (λ_1 in this paper) terminates at the RCP and is thus negative. The density is a minimum in the ring surface at the RCP, and thus, the two curvatures (λ_2 and λ_3 in this paper) in the ring surface or plane are positive and originate at the critical point (CP). For the BCP, one negative curvature (λ_1 in this paper) is directed perpendicular to the ring surface, the other one negative curvature (λ_2 in this paper) of the BCP lies in the plane of the ring, and the positive curvature (λ_3 in this paper) defines the bond path.

The transition structure on the IRC path for the reaction of A−B−C → B−C−A has been discussed,[23] it is always near the (energy) transition state. In the FNCX → FXCN (X = O, S, and Se) process, we still put the emphasis on the narrow area along the reaction path around the (energy) transition state.

In the FNCX → FXCN (X = O, S, and Se) process, the electronic density $\rho(\boldsymbol{r}_c)$ at the BCP of the F−N bond becomes smaller and smaller, which indicates that the F−N bond becomes weaker and weaker, and at last, it is broken. When the F−N bond is broken, the F−C bond forms, and the F−C bond becomes strongest at the point FCNX (IM). As the reactions proceed, $\rho(\boldsymbol{r}_c)$ at the BCP of the F−C bond becomes smaller and the F−X (X=O, S, and Se) bond becomes larger, which indicates that the F−C bond becomes weaker and the F−X (X = O, S, and Se) bond becomes stronger, and then FXCN (X = O, S, and Se) forms. As the reactions proceed, $\rho(\boldsymbol{r}_c)$ at the BCP of the N−C bond becomes somewhat larger, and $\rho(\boldsymbol{r}_c)$ at the BCP of the C−X (X=O, S, and Se) bond becomes somewhat smaller, which indicates that the N−C bond becomes somewhat stronger and the C−X (X = O, S, and Se) bond becomes somewhat weaker.

For the FNCO → FOCN process, from FNCO to the first energy transition state (TSa), the F−N bond becomes weaker and weaker, the bond path becomes more and more bent, and the F−N bond slides along the N−C bond. At the point $S_a = -2.20$, there is a bond path between the fluorine nucleus and the BCP of the N−C bond. After that point, the F−C bond forms. The F−C bond becomes straighter at the intermediate FCNO. From the intermediate FCNO to the second energy transition state (TSb), the F−C bond begins to slide along the C−O bond. At the point $S_b = -0.30$, there is a bond path between the fluorine nucleus and the BCP of C−O bond. After that point, the F−O bond forms and becomes stronger.

For the FNCS → FSCN process, from FNCS to the first energy transition state (TSa), the F−N bond path becomes more and more bent. At the point $S_a = -0.90$, there is a bond path between the fluorine nucleus and the BCP of the N−C bond. After that point, the F−C bond forms. The F−C bond becomes straighter at the intermediate FCNS. From the intermediate FCNS to the second energy transition state (TSb), the F−C bond

TABLE 4: (a) Electronic Densities $\rho(r_c)$ at the Critical Points on FNC → FSCN Pathway and (b) Topological Characters of BCP and RCP of the Ring Transition Region on FNCS → FSCN Pathway

(a)

$S^{a,b,c}$/(amu)$^{1/2}$bohr	F−N	F−BCP(N−C)	F−C	F−S	N−C	C−S
FNCS	0.2861				0.4289	0.2532
$S_a = -1.00$	0.1198				0.4366	0.2535
$S_a = -0.90$ (STS)		0.1213			0.4364	0.2527
$S_a = -0.80$			0.1233		0.4367	0.2517
$S_a = 0.00$ (TSa, ETS)			0.1525		0.4369	0.2412
IM			0.3040		0.4369	0.2003
$S_b = 0.00$ (TSb, ETS)			0.1153		0.4648	0.2514
$S_b = +1.78$			0.0683		0.4899	0.2479
$S_b = +1.79$			0.0682	0.0668	0.4899	0.2479
$S_b = +1.86$ (STS)			0.0675	0.0673	0.4903	0.2476
$S_b = +1.94$			0.0669	0.0681	0.4906	0.2473
$S_b = +1.95$				0.0682	0.4907	0.2473
FSCN				0.1858	0.4868	0.2251

(b)

			eigen. of the hess. matrix			
	S_b [a,c]/(amu)$^{1/2}$bohr	ρ	λ_1	λ_2	λ_3	$\nabla^2\rho$ [d]
RCP	+1.79	0.0668[e]	−0.0742	0.0042[e]	0.2966	0.2266
	+1.83	0.0670	−0.0759	0.0088	0.3071	0.2400
	+1.85	0.0670	−0.0765	0.0094	0.3115	0.2444
	+1.86(STS)	0.0670	−0.0769	0.0095	0.3137	0.2463
	+1.87	0.0670	−0.0772	0.0094	0.3161	0.2483
	+1.89	0.0670	−0.0778	0.0090	0.3209	0.2521
	+1.90	0.0670	−0.0782	0.0085	0.3236	0.2539
	+1.94	0.0669[f]	−0.0800	0.0033[f]	0.3397	0.2630
F−S bond	+1.79	0.0668[e]	−0.0729	−0.0046[e]	0.2875	0.2100
	+1.83	0.0671	−0.0725	−0.0127	0.2827	0.1975
	+1.85	0.0673	−0.0726	−0.0154	0.2815	0.1935
	+1.86(STS)	0.0674	−0.0726	−0.0166	0.2810	0.1918
	+1.87	0.0675	−0.0727	−0.0177	0.2807	0.1903
	+1.89	0.0677	−0.0728	−0.0198	0.2800	0.1874
	+1.90	0.0677	−0.0729	−0.0208	0.2797	0.1860
	+1.94	0.0681	−0.0732	−0.0244	0.2790	0.1814
F−C bond	+1.79	0.06817	−0.0869	−0.0223	0.3914	0.2822
	+1.83	0.06778	−0.0858	−0.0190	0.3849	0.2801
	+1.85	0.0676	−0.0852	−0.0171	0.3813	0.2790
	+1.86(STS)	0.0675	−0.0849	−0.0161	0.3794	0.2784
	+1.87	0.0674	−0.0846	−0.0151	0.3774	0.2777
	+1.89	0.0673	−0.0839	−0.0128	0.3730	0.2763
	+1.90	0.0672	−0.0835	−0.0115	0.3704	0.2754
	+1.94	0.0669[f]	−0.0816	−0.0035[f]	0.3548	0.2697

[a] S, reaction coordinate. [b] −, denotes reverse direction of the reaction. [c] +, denotes forward direction of the reaction. [d] $\nabla^2\rho$, Laplacian of electron density. [e] The formation of the ring structure with a singularity in the density. [f] The annihilation of the ring structure with a singularity in the density.

path becomes more and more bent. In the region of $S_b = +1.79 \rightarrow +1.94$, the RCP appears, and a F−C−S three-membered ring exists. From the point $S_b = +1.95$, the F−C bond disappears and then the F−S bond becomes stronger, and then FSCN forms.

For the FNCSe → FSeCN process, from FNCSe to the first energy transition state (TSa), the F−N bond path becomes more and more bent. At the point $S_a = -0.40$, there is a bond path between the fluorine nucleus and the BCP of N−C bond. After that point, the F−C bond forms. The F−C bond becomes straighter at the intermediate FCNSe. From the intermediate FCNSe to the second energy transition state (TSb), the F−C bond path becomes more and more bent. In the region of $S_b = +2.05 \rightarrow +2.66$, the RCP appears and a F−C−Se three-membered ring exists. From the point $S_b = +2.67$, the F−C bond disappears and the F−Se bond becomes stronger, and then FSeCN forms.

On the basis of the catastrophe theory,[10,11] Bader et al. pointed out that for a simple ABC system a two-dimensional cross-section of the structure diagram can be used to predict the existence of conflict-type and bifurcation-type mechanism.[8−12] In the bifurcation mechanism, the formation or annihilation of the ring structure occurs with the formation of a singularity in the density. At a singularity in the density, the first and second derivatives are zero and the CP has a rank less than 3; that is, it has a rank of two in the present case since there is one zero curvature. The singularity in the density is unstable, and for an infinitesimal increase in reaction coordinate, it bifurcates into a BCP and RCP. The negative curvature of the BCP lying in the plane will, like the associated curvature of the RCP, initially be close to zero. Initially, the BCP and RCP will have eigenvectors directed at one another: a positive one for the RCP, and a negative one for the BCP. They increase and decrease, respectively, from zero as the newly formed BCP and RCP separate. As the reaction gets to the point, where the BCP and RCP merge, another singularity is formed in the density: the point where a bond is broken. For points very close to the singularity, the two curvatures will be of almost equal magnitude and opposite signs.[11]

In the FNCS → FSCN process, there is a conflict structure during the migration of the F−N bond to the F−C bond, and a

TABLE 5: (a) Electronic Densities $\rho(r_c)$ at the Critical Points on FNCSe → FSeCN Pathway and (b) Topological Characters of the RCP on IRC Path of FNCSe → FSeCN

(a)

$S^{a,b,c}$/(amu)$^{1/2}$bohr	F−N	F−BCP(N−C)	F−C	F−Se	N−C	C−Se
FNCSe	0.2849				0.4306	0.2081
$S_a = -0.50$	0.1108				0.4473	0.2064
$S_a = -0.40$ (STS)		0.1123			0.4476	0.2052
$S_a = -0.30$			0.1141		0.4478	0.2038
$S_a = 0.00$(TSa, ETS)			0.1280		0.4490	0.1961
IM			0.3021		0.4410	0.1550
$S_b = 0.00$ (TSb, ETS)			0.1214		0.4677	0.1974
$S_b = +2.04$			0.0635		0.4905	0.1930
$S_b = +2.05$			0.0633	0.0573	0.4905	0.1929
$S_b = +2.35$ (STS)			0.0601	0.0589	0.4911	0.1920
$S_b = +2.66$			0.0569	0.0620	0.4919	0.1906
$S_b = +2.67$				0.0621	0.4918	0.1906
FSeCN				0.1563	0.4886	0.1757

(b)

			eigen. of the hess. matrix			
	S_b [a,c]/(amu)$^{1/2}$bohr	ρ	λ_1	λ_2	λ_3	$\nabla^2\rho$ [d]
RCP	+2.05	0.0572[e]	−0.0576	0.0045[e]	0.2270	0.1739
	+2.10	0.0574	−0.0586	0.0110	0.2306	0.1830
	+2.20	0.0576	−0.0600	0.0161	0.2365	0.1926
	+2.25	0.0576	−0.0606	0.0173	0.2396	0.1963
	+2.30	0.0576	−0.0611	0.0180	0.2428	0.1997
	+2.34	0.0576	−0.0615	0.0181	0.2455	0.2021
	+2.35(STS)	0.0576	−0.0616	0.0181	0.2462	0.2027
	+2.36	0.0576	−0.0617	0.0180	0.2470	0.2033
	+2.40	0.0575	−0.0621	0.0177	0.2500	0.2056
	+2.50	0.0575	−0.0630	0.0159	0.2578	0.2107
	+2.60	0.0572	−0.0639	0.0111	0.2699	0.2171
	+2.66	0.0569[f]	−0.0649	0.0040 [f]	0.2839	0.2230
F−Se bond	+2.05	0.0573[e]	−0.0568	−0.0047[e]	0.2242	0.1627
	+2.10	0.0575	−0.0567	−0.0123	0.2232	0.1542
	+2.20	0.0582	−0.0571	−0.0205	0.2235	0.1459
	+2.25	0.0585	−0.0575	−0.0236	0.2240	0.1429
	+2.30	0.0589	−0.0579	−0.0263	0.2247	0.1405
	+2.34	0.0592	−0.0582	−0.0283	0.2254	0.1389
	+2.35(STS)	0.0593	−0.0583	−0.0288	0.2256	0.1385
	+2.36	0.0594	−0.0584	−0.0293	0.2258	0.1381
	+2.40	0.0597	−0.0588	−0.0311	0.2266	0.1367
	+2.50	0.0606	−0.0598	−0.0353	0.2286	0.1335
	+2.60	0.0615	−0.0610	−0.0392	0.2312	0.1310
	+2.66	0.0620	−0.0617	−0.0413	0.2330	0.1300
F−C bond	+2.05	0.0633	−0.0801	−0.0397	0.3724	0.2526
	+2.10	0.0626	−0.0789	−0.0376	0.3675	0.2510
	+2.20	0.0613	−0.0764	−0.0334	0.3576	0.2478
	+2.25	0.0607	−0.0752	−0.0312	0.3527	0.2463
	+2.30	0.0601	−0.0741	−0.0290	0.3476	0.2445
	+2.34	0.0596	−0.0732	−0.0272	0.3436	0.2432
	+2.35(STS)	0.0596	−0.0730	−0.0267	0.3426	0.2429
	+2.36	0.0595	−0.0728	−0.0262	0.3416	0.2426
	+2.40	0.0591	−0.0720	−0.0242	0.3373	0.2411
	+2.50	0.0583	−0.0702	−0.0195	0.3274	0.2377
	+2.60	0.0574	−0.0680	−0.0122	0.3134	0.2332
	+2.66	0.0569 [f]	−0.0662	−0.0041[f]	0.2986	0.2283

[a] S, reaction coordinate. [b] −, denotes reverse direction of the reaction. [c] +, denotes forward direction of the reaction. [d] $\nabla^2\rho$, Laplacian of electron density. [e] The formation of the ring structure with a singularity in the density. [f] The annihilation of the ring structure with a singularity in the density.

bifurcation-type F−C−S ring structure appears in the migration of the fluorine atom for the formation of the F−S bond and annihilation of the F−C bond. The formation of the F−C−S three-membered ring structure occurs with the formation of a singularity in the density. That is, the density at the newly appeared BCP of the F−S bond and the RCP of the F−C−S ring is the same value at the point of $S_b = +1.79$. From Table 4b, λ_2 eigenvalues (the negative curvature lying in the plane) of the BCP of the F−S bond and the associated curvature of the RCP of the F−C−S ring structure have almost equal magnitude and opposite signs. In the region of $S_b = +1.79 \rightarrow +1.94$, λ_2 eigenvalues of the F−S BCP and RCP decrease and increase, respectively. After the point $S_b = +1.86$, the λ_2 eigenvalue of the RCP begins to decrease. At the point $S_b = +1.94$, the BCP of the F−C bond and the RCP merge to form another singularity in the density, where the F−C bond is broken. (Table 4b, the two curvatures have almost equal magnitude and opposite signs).

The FNCSe → FSeCN process is similar to the FNCS→FSCN process: there is a conflict structure in the migration of the

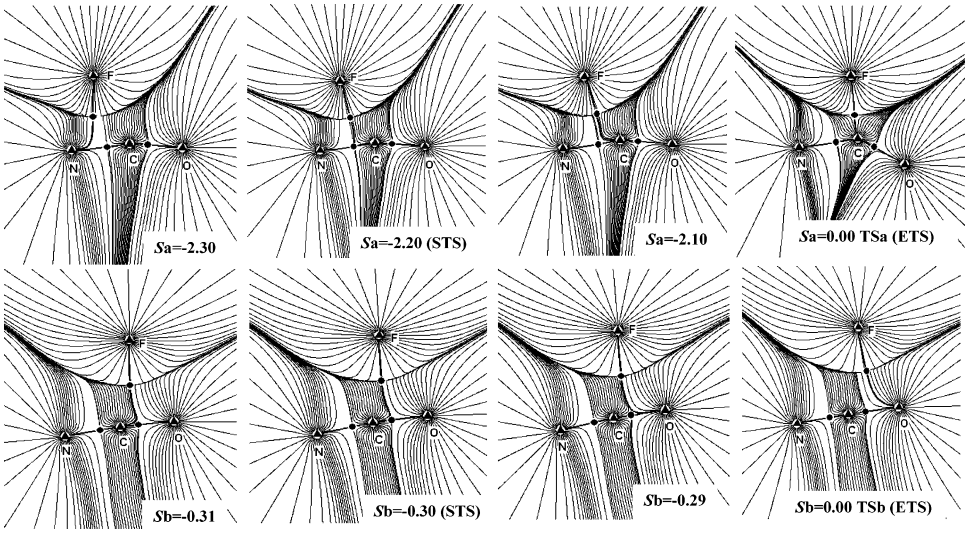

Figure 3. Gradient paths of the electronic density on the IRC path of FNCO → FOCN. Triangle denotes nuclei, circle denotes BCP and rectangle denotes RCP.

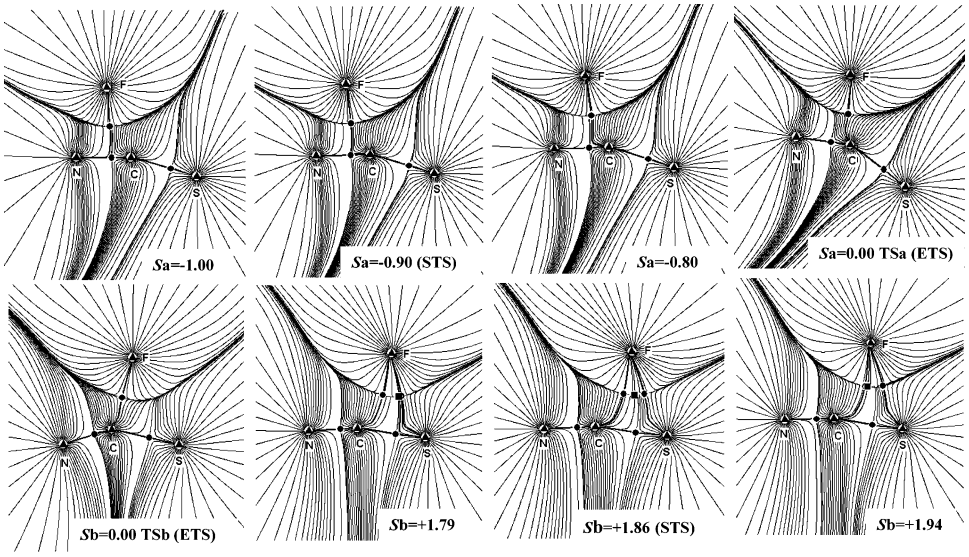

Figure 4. Gradient paths of the electronic density on the IRC path of FNCS → FSCN. Triangle denotes nuclei, circle denotes BCP and rectangle denotes RCP.

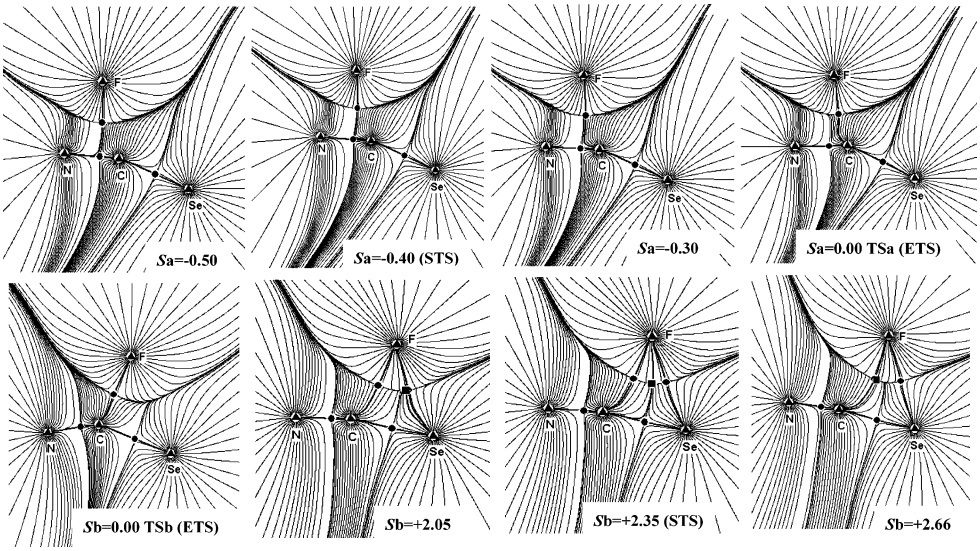

Figure 5. Gradient paths of the electronic density on the IRC path of FNCSe → FSeCN. Triangle denotes nuclei, circle denotes BCP and rectangle denotes RCP.

F−N bond to the F−C bond and a bifurcation-type F−C−Se ring structure appears in the migration of the fluroine atom to form the F−Se bond. Both the formation and annihilation of the F−C−Se three-membered ring structure occur with the formation of a singularity in the density (Table 5-b: $Sb = +2.05$ of the F−Se BCP and the RCP, $Sb = +2.66$ of the F−C BCP and the RCP, the two curvatures are of almost equal magnitude and opposite signs).

3.2.2. Structure Transition State and the Structure Transition Region. When a bond is broken and a new bond is formed, the "structure transition state" and "structure transition region" will appear. One is a kind of T-shaped conflict structure transition state that includes a bond path linking a nucleus and a bond critical point (BCP). We call it "the first kind of structure transition state". The other one is a kind of bifurcation-type ring structure transition region enveloped by some bond paths and three or more nuclei. As the ring critical point (RCP) appears, it is very close to the BCP of the newly formed bond. As the process proceeds, the RCP moves to the center of the ring. When the RCP goes near the BCP of another bond, this bond is broken, and the ring disappears. From the ring's appearance to disappearance, the λ_2 eigenvalue of the Hessian matrix of RCP (the positive curvature lying in the plane) has the trends of zero (close to zero) → maximum → zero (close to zero). We define the point corresponding to the maximum of the Hessian matrix λ_2 value as "the second kind of structure transition state" of the bifurcation-type ring structure transition region. We call the T-shaped conflict-type transitional structure or bifurcation-type ring transitional structure as structure transition state (STS). For clarity, the traditional transitional state that is the maximum on the energy surface is called "energy transition state" (ETS).

Both kinds of structure transition states appear in the FNCX → FXCN (X = O, S, and Se) process. $S_a = -2.20$ and $S_b = -0.30$ for the FNCO → FOCN process, $S_a = -0.90$ for the FNCS → FSCN process, and $S_a = -0.40$ for the FNCSe → FSeCN process all are T-shaped conflict-type STS. The regions of $S_b = +1.79 \rightarrow +1.94$ for the FNCS → FSCN process and $S_b = +2.05 \rightarrow +2.66$ for the FNCSe → FseCN process are bifurcation-type ring structure transition regions. The three-membered ring STSs of the structure transition regions are $S_b = +1.86$ and $+2.35$ for the FNCS→FSCN and FNCSe → FSeCN processes, respectively.

Figure 2 also gives the position of the STS and ETS along the reaction pathways. The positions of the STS are $S_a = -2.20$ and $S_b = -0.30$ for FNCO → FOCN process, $S_a = -0.90$ and $S_b = +1.86$ for FNCS → FSCN process, and $S_a = -0.40$ and $S_b = +2.35$ for FNCSe → FSeCN process, respectively. That is, the position of the STS appears later and later according to the sequence of O, S, and Se. There is no ring STS for the FNCO → FOCN process, the ranges of the ring structure regions are $S_b = +1.79 \rightarrow +1.94$ for the FNCS → FSCN process and $S_b = +2.05 \rightarrow +2.66$ for the FNCSe → FSeCN process. That is, the range of the ring structure regions becomes wider and wider in the sequence of O, S, and Se. The sulfur and selenium atoms have much larger van der Waals and covalent radii than oxygen, which can explain the sequence of the width of the ring structure transition regions.

4. Conclusions

(1) There are two steps in each of the topic reactions: the first step is FNCX → TSa → IM and the second step is IM → TSb → FXCN (X = O, S, and Se). The geometries of the intermediates and the transition states of the reactions studied are found for the first time.

(2) The Gibbs free energy changes of the FNCO → FCNO(IM) and FCNO(IM) → FOCN processes are both less than zero, and the Gibbs free energy changes of the FNCX → FCNX(IM) and FCNX(IM) → FXCN (X=S, and Se) processes are both more than zero. The FNCO → FCNO process is difficult, and the processes of FNCX → FXCN (X=S and Se) are easy. Therefore, FSCN instead of FNCS is easily detected in the experiments, and we predict that FNCO and FSeCN are more easily detected than FOCN and FNCSe, respectively.

(3) There are two kinds of STS in the topic reactions, the T-shaped conflict STS and the three-membered ring STS. In the ring structure transition region, from the ring's appearance to disappearance, the λ_2 eigenvalue (the positive curvature lying in the plane) of the Hessian matrix of the RCP has the trends of zero → maximum → zero. We define the point corresponding to the maximum of the Hessian matrix λ_2 value as "the second kind of structure transition state" of the bifurcation-type ring transition region.

(4) The position of the STS on the reaction path appears later and later according to the sequence of O, S, and Se; the range of the ring structure regions also becomes more and more wide also in the sequence of O, S, and Se.

Acknowledgment. This project was supported by the Nature Science Foundation of Hebei Province (Contract No. B2004000147). Y.Z. thanks the Chinese Academy of Sciences for a scholarship during the period of this work. The authors also thank Prof. Wang Dianxun for his helpful discussions in this work.

References and Notes

(1) Frost, D. C.; Kroto, H. W.; McDowell, C. A.; Westwood, N. P. C. *J. Electron Spectrosc. Relat. Phenom.* **1977**, *11*, 147.
(2) Frost, D. C.; MacDonald, C. B.; McDowell, C. A.; Westwood, N. P. C. *Chem. Phys.* **1980**, *47*, 111.
(3) Li, Y. M.; Qiao, Z. M.; Sun, Q.; Zhao, J. C.; Li, H. Y.; Wang, D. X. *Inorg. Chem.* **2003**, *42* (25), 8846.
(4) Jonkers, G.; Grabandt, O.; Mooyman, R.; de Lange, C. A. *J. Electron Spectrosc. Relat. Phenom.* **1982**, *26*, 147.
(5) Frost, D. C.; MacDonald, C. B.; McDowell, C. A.; Westwood, N. P. C. *J. Am. Chem. Soc.* **1981**, *103*, 4423.
(6) Leung, H.; Suffolk, R. J.; Watts, J. D. *Chem. Phys.* **1986**, *109*, 289.
(7) Jonkers, G.; Mooyman, R.; de Lange. C. A. *Mol. Phys.* **1981**, *43*, 655.
(8) Bader, R. F. W.; Nguyen-Dang, T. T.; Tal, Y. *J. Chem. Phys.* **1979**, *70* (9), 4316.
(9) Tal, Y.; Bader, R. F. W.; Nguyen-Dang, T. T. *J. Chem. Phys.* **1981**, *74*, 5162.
(10) Bader, R. F. W.; Nguyen-Dang, T. T.; Tal, Y. *Rep. Prog. Phys.* **1981**, *44*, 893.
(11) Bader, R. F. W. *Atoms in Molecules—A Quantum Theory*; Oxford University Press: Oxford, U.K., 1990.
(12) Bader, R. F. W.; Tang, T.-H.; Tal, Y. Biegler-König F. W. *J. Am. Chem. Soc.* **1982**, *104*, 946.
(13) Popelier, P. *Atoms in Molecules-An Introduction*, UMIST, Manchester, UK. **2000**.
(14) Vyboishchikov S. F.; Masunov, A. E. *J. Mol. Struct. (THEOCHEM)* **1994**, *311*, 161.
(15) Alikhani, M. E.*Chem. Phys. Lett.* **1997**, *277*, 239.
(16) Dixon, R. E.; Streitwieser A.; Laidig, K. E.; Bader, R. F. W.; Harder S. *J. Phys. Chem.* **1993**, *97*, 3728.
(17) Zheng, S. J.; Meng, L. P.; Cai, X. H.; Xu, Z. F.; Fu, X. Y. *J. Comput. Chem.* **1997**, *18*, 1167.
(18) Ishida, K.; Morokuma, K.; Komornicki. A. *J. Chem. Phys.* **1977**, *66*, 2153.
(19) Gonzalez, C.; Schlegel, H. B. *J. Chem. Phys.* **1989**, *90*, 2154.
(20) Gonzalez, C.; Schlegel, H. B. *J. Phys. Chem.* **1990**, *94*, 5523.
(21) Frisch, M. J.; Trucks, G. W.; Schlegel, H. B.; Scuseria, G. E.; Robb, M. A.; Cheeseman, J. R.; Zakrzewski, V. G.; Montgomery, J. A., Jr.; Stratmann, R. E.; Burant, J. C.; Dapprich, S.; Millam, J. M.; Daniels, A. Stratmann, R. E.; Burant, J. C.; Dapprich, S.; Millam, J. M.; Daniels, A. D.; Kudin, K. N.; Strain, M. C.; Farkas, O.; Tomasi, J.; Barone, V.; Cossi,

M.; Cammi, R.; Mennucci, B.; Pomelli, C.; Adamo, C.; Clifford, S.; Ochterski, J.; Petersson, G. A.; Ayala, P. Y.; Cui, Q.; Morokuma, K.; Malick, D. K.; Rabuck, A. D.; Raghavachari, K.; Foresman, J. B.; Cioslowski, J.; Ortiz, J. V.; Stefanov, B. B.; Liu, G.; Liashenko, A.; Piskorz, P.; Komaromi, I.; Gomperts, R.; Martin, R. L.; Fox, D. J.; Keith, T.; Al-Laham, M. A.; Peng, C. Y.; Nanayakkara, A.; Gonzalez, C.; Challacombe, M.; Gill, P. M. W.; Johnson, B. G.; Chen, W.; Wong, M. W.; Andres, J. L.; Head-Gordon, M.; Replogle, E. S.; Pople, J. A. *Gaussian 98*, revision A.3; Gaussian, Inc.: Pittsburgh, PA, 1998.

(22) Biegler-König, F. AIM 2000 version 1.0; University of Applied Science: Bielefeld, Germany, 1998−2000.

(23) Bader, R. F. W. *Chem. Rev.* **1991**, *91*, 1 (5), 893.